A Conserved PP2A Regulatory Subunit Enforces Proportional Relationships Between Cell Size and Growth Rate

Ricardo M. Leitao, Akshi Jasani, Rafael A. Talavera, Annie Pham, Quincy J. Okobi, and Douglas R. Kellogg[1]

Department of Molecular, Cell and Developmental Biology, University of California, Santa Cruz, California 95064

ORCID IDs: 0000-0002-0916-7945 (R.M.L.); 0000-0002-5835-4691 (A.J.); 0000-0002-1610-9153 (R.A.T.); 0000-0001-9925-2600 (Q.J.O.); 0000-0002-5050-2194 (D.R.K.)

ABSTRACT Cell size is proportional to growth rate. Thus, cells growing rapidly in rich nutrients can be nearly twice the size of cells growing slowly in poor nutrients. This proportional relationship appears to hold across all orders of life, yet the underlying mechanisms are unknown. In budding yeast, most growth occurs during mitosis, and the proportional relationship between cell size and growth rate is therefore enforced primarily by modulating growth in mitosis. When growth is slow, the duration of mitosis is increased to allow more time for growth, yet the amount of growth required to complete mitosis is reduced, which leads to the birth of small daughter cells. Previous studies have found that Rts1, a member of the conserved B56 family of protein phosphatase 2A regulatory subunits, works in a TORC2 signaling network that influences cell size and growth rate. However, it was unclear whether Rts1 influences cell growth and size in mitosis. Here, we show that Rts1 is required for the proportional relationship between cell size and growth rate during mitosis. Moreover, nutrients and Rts1 influence the duration and extent of growth in mitosis via Wee1 and Pds1/securin, two conserved regulators of mitotic progression. Together, the data are consistent with a model in which global signals that set growth rate also set the critical amount of growth required for cell cycle progression, which would provide a simple mechanistic explanation for the proportional relationship between cell size and growth rate.

KEYWORDS cell growth; cell size; Pds1; PP2A; Rts1; securin; Swe1; Wee1

A critical step in the evolution of life was attainment of the capacity for growth. Along with growth, early cells must have evolved mechanisms to control growth if they were to survive and compete. Thus, early cells likely evolved mechanisms to control the rate and extent of membrane growth and ribosome biogenesis, and to match the rates of each process to each other and to the availability of building blocks derived from nutrients. Mechanisms that control growth ultimately determine the size and shape of a cell, and are responsible for the myriad sizes, shapes, and growth rates observed in cells spanning all orders of life.

doi: https://doi.org/10.1534/genetics.119.301012
Manuscript received February 26, 2019; accepted for publication August 10, 2019; published Early Online September 3, 2019.
Supplemental material available at FigShare: https://doi.org/10.25386/genetics.9701960.
[1]Corresponding author: Department of Molecular, Cell and Developmental Biology, University of California, 1156 High Street, Santa Cruz, CA 95064. E-mail: dkellogg@ucsc.edu

Growth of budding yeast during the cell cycle illustrates how mechanisms that control cell growth define the size and shape of cells. Growth occurs in distinct phases that are characterized by different rates and patterns of growth (Johnston *et al.* 1977; McCusker *et al.* 2007; Goranov *et al.* 2009; Ferrezuelo *et al.* 2012; Leitao and Kellogg 2017). During G1 phase, growth occurs at a slow rate over the entire surface of the cell. At the end of G1 phase, growth of the mother cell ceases and polarized growth of a daughter bud is initiated. Entry into mitosis triggers a switch to isotropic growth that occurs over the entire bud surface and the rate of growth increases two-to-threefold. Rapid growth continues throughout mitosis and accounts for most of the volume of a yeast cell (Leitao and Kellogg 2017). Thus, only 20% of the volume of a new mother cell is achieved during the previous G1 phase, while $>$ 60% of the volume is achieved during the previous mitosis. The volume achieved during G1 phase increases to ~40% under conditions of poor nutrients. The distinct size and shape of a budding yeast cell is ultimately

defined by mechanisms that control the location and extent of growth during each of these growth phases.

The amount of growth that occurs during the cell cycle is influenced by growth rate. For example, yeast cells growing slowly in poor nutrients are nearly one-half the size of cells in rich nutrients (Johnston *et al.* 1977; 1979). This observation illustrates a poorly understood aspect of growth control: cell size is proportional to growth rate (Ferrezuelo *et al.* 2012; Leitao and Kellogg 2017). The relationship holds when comparing cells growing under different nutrient conditions that support different growth rates, and also when comparing cells that show different growth rates despite growing under identical nutrient conditions. Conversely, the growth rate of the daughter bud is proportional to the size of the mother cell, which shows that growth rate can be proportional to cell size (Elliott and McLaughlin 1978; Schmoller *et al.* 2015; Leitao and Kellogg 2017). Proportional relationships between cell size and growth rate appear to hold across all orders of life (Schaechter *et al.* 1958; Robertson 1963; Hirsch and Han 1969; Fantes and Nurse 1977; Johnston *et al.* 1977; Tzur *et al.* 2009).

Clues to a mechanistic basis for the relationship between cell size and growth rate in budding yeast have come from analysis of Rts1, a conserved regulatory subunit for protein phosphatase 2A (PP2A) (Shu *et al.* 1997). Rts1 forms a complex with PP2A that we refer to as $PP2A^{Rts1}$. Rts1 may also associate with Glc7, the budding yeast homolog of protein phosphatase 1 (Castermans *et al.* 2012). Early studies established that Rts1 is required for normal control of cell growth and size (Artiles *et al.* 2009; Zapata *et al.* 2014). Thus, cells that lack Rts1 are abnormally large and fail to modulate their size in response to changes in nutrient availability. Further analysis led to the discovery that Rts1 relays signals that control a TORC2 signaling network that is required for normal control of growth rate and cell size (Lucena *et al.* 2018). A key function of the TORC2 network is to control the synthesis of ceramide lipids, which play roles in signaling and may be the critical output of the TORC2 network that influences cell growth and size. Cells that cannot synthesize ceramides show a failure in nutrient modulation of cell size, as well as a failure to match growth rate to nutrient availability in G1 phase. Together, the data thus far suggest a model in which TORC2-dependent signals that set growth rate also set the threshold amount of growth required for cell cycle progression, which would provide a simple mechanistic explanation for the proportional relationship between cell size and growth rate. However, the mechanisms by which the TORC2 network influence cell growth and size are poorly understood, and it is unclear whether the network influences growth during the mitotic growth interval.

The proportional relationship between cell size and growth rate holds during bud growth (Leitao and Kellogg 2017). Thus, cells growing slowly in poor nutrients complete mitosis at a dramatically reduced daughter cell size. Early studies suggested that reduced daughter cell size in poor nutrients is a consequence of a timer mechanism that sets an invariant duration of bud growth (Hartwell and Unger 1977). In this model, cell size at completion of mitosis would be a simple outcome of the rate of growth during an invariant time interval. However, more recent analysis found that the duration of bud growth is not invariant (Leitao and Kellogg 2017). Rather, the duration of bud growth in mitosis is increased when growth is slowed by poor nutrients, which suggests that cells compensate for slow growth by increasing the duration of growth to ensure that sufficient growth occurs before the completion of mitosis. The data suggest that the duration and extent of bud growth are tightly controlled to maintain a specific cell size. A key step in testing this model is to identify proteins that influence the duration and extent of bud growth.

Here, we have initiated a search for proteins that influence cell size by controlling the duration and extent of bud growth in mitosis. A number of observations suggest that TORC2-dependent signals influence cell growth and size in mitosis. For example, the extent of growth in mitosis is dramatically reduced in mutants that have reduced TORC2-dependent signaling. This can be seen as a reduction in the size of the smallest cells in a population, which represent newborn cells that have just completed mitosis (Lucena *et al.* 2018). Moreover, a proteome-wide mass spectrometry search for proteins controlled by $PP2A^{Rts1}$, an important regulator of the TORC2 network, identified numerous proteins implicated in the control of mitotic progression and cell size (Zapata *et al.* 2014). Therefore, to investigate further we first tested whether Rts1 influences cell growth and size in mitosis.

Materials and Methods

Yeast strains and media

The genotypes of the strains used in this study are listed in Table 1. All strains are in the W303 background (leu2-3,112 ura3-*1 can1-100 ade2-1 his3-11,15 trp1-1 GAL+*, *ssd1-d2*). Genetic alterations were carried out using one-step PCR-based integration at the endogenous locus (Longtine *et al.* 1998; Janke *et al.* 2004) or by genetic crossing. Auxin-inducible degron (AID) strains were created as previously described (Nishimura *et al.* 2009). TIR1-containing plasmids (pTIR2 and pTIR4) were integrated into strain DK186, and the AID::-KanMX6 cassette was amplified from pAID_C and integrated at the C-terminus of *RTS1*.

pds1-4A mutants were created by replacing a 170-bp fragment of *PDS1* that contains S185, S186, S212, and S213 with the *URA3* marker. The replacement was carried out in a PDS1-*3xHA*::*TRP* strain so that the final mutant version of *PDS1* would be tagged with 3XHA. The *URA3* marker gene was replaced by a mutant fragment of *PDS1* in which all four sites were mutated to alanine, which was synthesized by overlap PCR. The mutant fragment was cotransformed with a *LEU2*-marked *CEN* vector (YCplac111) and LEU + transformants were selected to enrich for transformation-competent

Table 1 Genotypes of yeast strains used in this study

Strain	Mating type	Genotype
DK186	*MAT***a**	*bar1*
DK2423	*MAT***a**	*bar1 TIR1::LEU2 TIR1::HIS3 rts1-AID::KanMX6*
DK2523	*MAT***a**	*bar1 SPC42-GFP::HIS3 MYO1-GFP::TRP*
DK2879	*MAT***a**	*bar1 TIR1::LEU2 TIR1::HIS3 SPC42-GFP::hphNT1 MYO1-GFP:KITRP rts1-AID::KanMX6*
DK2930	*MAT***a**	*bar1 SPC42-GFP::HIS3, MYO1-GFP::TRP swe1Δ::URA3*
DK3072	*MAT***a**	*bar1 TIR1::LEU2, TIR1::HIS3, SPC42-GFP::hphNT1 MYO1-GFP::KITRP rts1-AID::KanMX6 swe1Δ::URA3*
DK1993	*MAT***a**	*bar1 GAL1-CDC20::NatNT2*
DK2176	*MAT***a**	*bar1 GAL1-CDC20::NatNT2 rts1Δ::KanMX6*
DK2243	*MAT***a**	*bar1 GAL1-CDC20::NatNT2 rts1Δ::KanMX6 swe1::URA3*
DK1140	MATα	*bar1 rts1Δ::HIS3*
DK647	*MAT***a**	*bar1 rts1Δ::KanMX6*
SH24	*MAT***a**	*bar1 swe1Δ::URA3*
DK3365	*MAT***a**	*bar1 rts1Δ::HIS swe1Δ::URA3*
DK1778	*MAT***a**	*bar1 PDS1-3XHA::TRP*
DK2678	*MAT***a**	*bar1 PDS1-3XHA::TRP rts1Δ::KanMX6*
DK3318	*MAT***a**	*bar1 pds1-4A-3XHA::TRP*
DK3316	*MAT***a**	*bar1 pds1-4A-3XHA::TRP rts1Δ::KanMX6*
DK815	MATα	*bar1 swe1Δ::URA3 rts1Δ::KanMX6*
DK3334	*MAT***a**	*bar1 pds1-4A-3XHA::TRP SPC42-GFP::HIS3*
DK3335	*MAT***a**	*bar1 pds1-4A-3XHA::TRP swe1Δ::URA3 SPC42-GFP::HIS3*

cells. The *LEU* + transformants were then replica plated to 5-FOA to select for cells that lost the *URA3* marker. Preselection for the LEU2 *CEN* vector dramatically reduced the background of spontaneous *ura3* mutants. The resulting strain was backcrossed once to wild-type and then to DK815 to obtain DK3320, which was transformed with SPC42-GFP::HIS to obtain DK3335.

For cell cycle time courses and analysis of cell size by Coulter counter, cells were grown in YP media (1% yeast extract, 2% peptone, and 40 mg/liter adenine) supplemented with 2% dextrose (YPD), or with 2% glycerol and 2% ethanol. For microscopy, cells were grown in complete synthetic media (CSM) supplemented with 2% dextrose (CSM-Dex), or 2% glycerol and 2% ethanol (CSM-G/E).

Microscopy and image analysis

Microscopy, image analysis, statistical analysis of microscopy data, and analysis of the durations of mitotic stages were carried out as previously described (Leitao and Kellogg 2017). Briefly, the duration of mitotic stages was determined by measuring the distance between GFP-marked mitotic spindle poles as a function of time. In early mitosis, Cdk1 triggers formation of a short spindle in which the spindle poles are separated by a distance of 1–2 μm, which is thought to correspond to metaphase (Fitch *et al.* 1992; Winey and O'Toole 2001). Therefore, we define the duration of metaphase as the interval when spindle poles are separated by 1–2 μm within the mother cell. Initiation of anaphase is detected when spindle poles begin to move further apart and one pole migrates into the daughter cell. We defined the duration of anaphase as the interval between anaphase initiation and the time when the spindle poles reach their maximum distance apart. In addition to the stages of mitosis, we defined an S/G2 interval as the time from bud emergence to spindle pole separation.

The microscopy data in Figure 3 and Figure 4 were generated using a Zeiss ([Carl Zeiss], Thornwood, NY) LSM 5 Pascal microscope as previously described (Leitao and Kellogg 2017). The microscopy data in Supplemental Material, Figure S4 were acquired on a Zeiss LSM 880 AiryScan microscope using a Plan-Apochromat 63×/1.4 n.a. oil objective. The microscope was equipped with an enclosed heat-block stage and the microscope was enclosed within a temperature-controlled chamber. Prior to imaging, the microscope was allowed to equilibrate to 27° for ≥ 1 hr. Optical sections were taken for a total of 14 z-planes every 0.37 μm, with frame averaging set to 2, to reduce noise. Images were acquired every 2 min and a total of two fields of view were recorded per strain during each imaging session. Zoom and frame size were set to 0.8× magnification to achieve a consistent pixel area of 1024 × 1024 pixels in XY, and pixel dwell time was 0.5 μsec. Laser power (488 nm) was set to 0.2% and the 561-nm laser power was set to 1% to minimize cell damage. The gains for GFP, red fluorescent protein, and bright-field microscopy were set to 550, 750, and 325, respectively. GFP signal was acquired on a gallium arsenide phosphide (GaAsP). detector and collected using a 498–548-nm band pass filter. Bright-field images were collected simultaneously.

Statistical analysis

Data acquired from ImageJ were analyzed using Apple Numbers, R (R Core Team 2016), RStudio (RStudio Team 2015), and the R package ggplot2 (Wickham 2009). *P*-values were calculated using Welch's two-sample *t*-test and a 95% C.I.

Cell cycle time courses, western blotting, and coulter counter analysis

Cell cycle time courses utilizing cells arrested in G1 phase with α factor were carried out as previously described (Harvey *et al.* 2011). To arrest cells in mitosis, *GAL1-CDC20* cells were grown overnight in YP media containing 2% raffinose and 2% galactose, and arrested by washing into YP containing 2%

raffinose. Cells were monitored until most cells had large buds. Cells were released from metaphase by readdition of 2% galactose. SDS-PAGE and western blotting were carried out as previously described (Harvey *et al*. 2011). Blots were probed overnight at 4° with affinity-purified rabbit polyclonal antibodies raised against Swe1 or with a phospho-specific antibody that recognizes Cdk1 phosphorylated at tyrosine 19 (10A11 #Cat; Cell Signaling Technology). Blots were exposed to film or imaged using a ChemiDoc MP System (Bio-Rad, Hercules, CA). For quantification of rts1-AID degradation, band intensities were quantified using ImageLab. Destruction of Rts1-AID was initiated by addition of 1 mM auxin from a 50-mM stock made in 100% ethanol.

For PhosTag western blots, cells were lysed by bead beating into sample buffer without phosphatase inhibitors. After cell lysis, samples were centrifuged for 1 min at 13,000 rpm at 4° and quickly placed in a boiling water bath for 7 min. Samples were loaded into 10% SDS-PAGE gels supplemented with 70 μM PhosTag and 140 μM $MnCl_2$. To prepare PhosTag gels, the gel mixture was degassed for 5 min prior to the addition of TEMED and polymerization was allowed to occur for 1–2 hr at room temperature followed by overnight at 4°. Gels were run at 10 mA for 6 hr until a 29-kDa marker was at the bottom of the gel. The gel was incubated for 10 min in transfer buffer supplemented with 2 mM EDTA, followed by a second incubation without EDTA. Gels were transferred onto nitrocellulose via the Trans-Blot Turbo Transfer System (Bio-Rad). Blots were probed at room temperature with the 12CA5 anti-HA monoclonal antibody followed by HRP-conjugated anti-mouse secondary antibody. Secondary antibodies were detected via chemiluminescence using Quantum substrate (Advansta). Analysis of cell size by Coulter counter was carried out as previously described (Leitao and Kellogg 2017).

Reproducibility

All experiments were carried out for a minimum of three biological replicates that yielded reproducible results.

Data availability

All data are provided in the manuscript. For live-cell analysis, data for all cells are provided in the dot plots shown in the supplemental figures. Tables that show numerical values for the data that were used to generate the dot plots are available upon request. Supplemental material available at FigShare: https://doi.org/10.25386/genetics.9701960.

Results

Rts1 is required for the proportional relationship between cell size and growth rate in mitosis

We first tested how inactivation of Rts1 influences mitotic duration and daughter cell size. Previous studies have shown that mother cell size strongly influences daughter cell size and growth rate (Johnston *et al.* 1977; Schmoller *et al.* 2015; Leitao and Kellogg 2017). Therefore, interpretation of results from *rts1*Δ cells would be complicated by the possibility that effects on bud growth and size are a secondary consequence of defects in mother cell size that arose in previous generations. To avoid this problem, we fused *RTS1* to an auxin-inducible degron (*rts1-AID*), which allowed us to observe the immediate effects of inactivating Rts1 (Nishimura *et al.* 2009). In the absence of auxin, *rts1-AID* did not cause defects in cell size or cell cycle progression (Figure S1, A and B). Addition of auxin caused rapid destruction of Rts1-AID protein within 15–30 min (Figure S1C). In the presence of auxin, ~10% of the Rts1-AID protein persisted and *rts1-AID* cells grown in auxin at elevated temperatures formed colonies more rapidly than *rts1*Δ cells (Figure S1D). Together, these observations show that *rts1-AID* causes a partial loss-of-function in the presence of auxin. Nevertheless, we utilized *rts1-AID* because it allowed analysis of bud growth and mitotic duration without the complication of aberrant mother cell size.

We used a microscopy-based assay (Ferrezuelo *et al.* 2012; Leitao and Kellogg 2017) to test how inactivation of *rts1-AID* influences the duration and extent of growth during metaphase and anaphase (see *Materials and Methods* for the criteria used to define the intervals of metaphase and anaphase). Cells were released from a G1-phase arrest and auxin was added shortly after bud emergence. Destruction of the Rts1-AID protein caused a threefold increase in the average duration of metaphase and anaphase, in both rich and poor carbon (Figure 1A; see Figure S2A for dot plots and *P*-values). Destruction of Rts1-AID also caused a large increase in the variance of metaphase duration compared to wild-type cells (Figure S2A).

We next analyzed daughter bud size at each mitotic transition. *rts1-AID* caused a large increase in daughter bud size at the completion of each stage of mitosis in both rich and poor carbon (Figure 1B; see Figure S2, C and D for dot plots and *P*-values). The variance in size at the end of metaphase was much larger in *rts1-AID* cells compared to wild-type cells (Figure S2C). In contrast to wild-type cells, there was not a statistically significant difference in the size of *rts1-AID* daughter cells between rich or poor carbon at the end of metaphase (Figure S2C). By the end of anaphase, *rts1-AID* cells in rich carbon were slightly larger than their counterparts in poor carbon (Figure S2D).

Further analysis of the *rts1-AID* allele led to surprising insight into the role of Rts1 in cell size control. Destruction of Rts1-AID reduced the average rate of growth in mitosis by ~30% in both rich and poor carbon (Figure 1C). In normal cells, reduced growth rate causes reduced cell size; however, destruction of Rts1-AID caused an increase in size. In addition, the correlation between growth rate and cell size was broken in *rts1-AID* cells (Figure 1D). Thus, buds with nearly identical growth rates completed mitosis at very different sizes. Conversely, cells that completed mitosis at identical sizes grew at very different rates during mitosis.

To summarize, a partial loss of Rts1 function caused major defects in cell size control in mitosis, as well as a loss of the proportional relationship between cell size and growth rate. As a next step, we sought to identify proteins that respond to

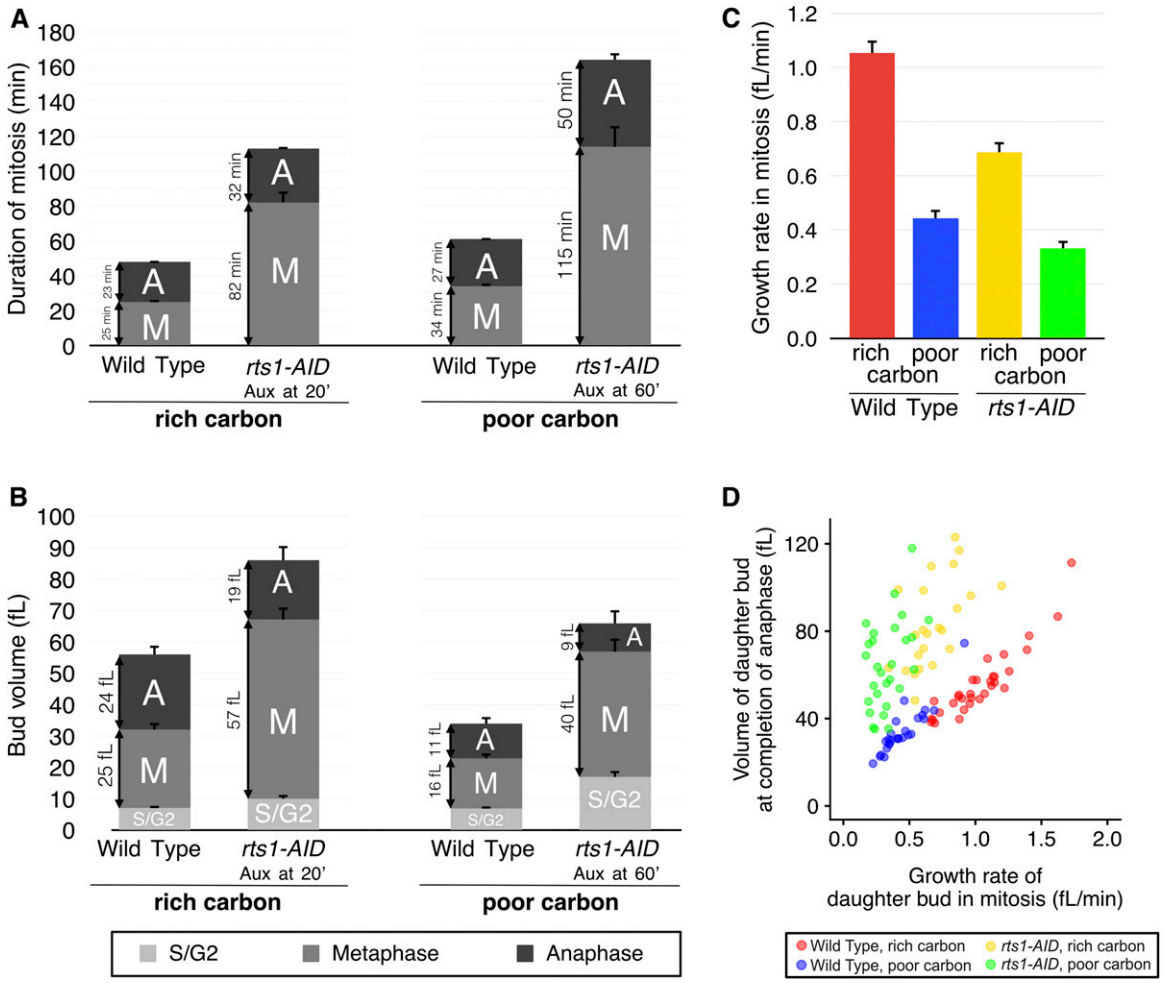

Figure 1 PP2A^{Rts1} is required for normal control of mitotic duration and cell size. (A) Plots showing the average durations of metaphase and anaphase for wild-type and *rts1-AID* cells, growing in rich or poor carbon. (B) The average growth in volume for all phases of the cell cycle except G1 phase is plotted for wild-type and *rts1-AID* cells, growing in rich or poor carbon. Due to the extended length of the cell cycle in *rts1-AID* cells, only a few cells could be followed through G1. For this reason, the limited data regarding G1 phase were omitted. (C) The growth rate during metaphase and anaphase was calculated as the average of individual cell growth rates. (D) A plot of the volume of the daughter bud at completion of anaphase *vs.* growth rate during metaphase plus anaphase. Error bars represent SEM. AID, auxin-inducible degron; PP2a, protein phosphatase 2A.

the PP2A^{Rts1}-dependent signals that control the duration of growth in mitosis. Over the long-term, identification of these proteins and the signals that control their activity should yield insight into the mechanisms that control cell growth and size.

Swe1 and Pds1 are candidate targets of Rts1-dependent control of cell growth in mitosis

We used a candidate approach to identify proteins that control the duration of growth in mitosis. To identify candidates, we used two criteria. First, we considered proteins that were previously found to control cell size and/or the duration of mitosis. Second, we considered potential targets of PP2A^{Rts1}-dependent regulation that were previously identified by proteome-wide mass spectrometry analysis of *rts1*Δ cells or by phenotypic analysis of *rts1*Δ cells (Harvey *et al.* 2011; Zapata *et al.* 2014). Two candidates fulfilled both criteria: Swe1 and Pds1/securin.

Swe1 is the budding yeast homolog of the Wee1 kinase, which phosphorylates and inhibits mitotic Cdk1. Loss of Swe1 causes reduced cell size (Jorgensen *et al.* 2002; Harvey and Kellogg 2003; Harvey *et al.* 2005). Wee1 family members were originally found to control mitotic entry; however, more recent studies have shown that Wee1 family members also play roles after mitotic entry and influence the duration of metaphase (Deibler and Kirschner 2010; Harvey *et al.* 2011; Lianga *et al.* 2013; Raspelli *et al.* 2015; Toledo *et al.* 2015). Moreover, Wee1 family members work in a systems-level mechanism that restrains full activation of Cdk1 in early mitosis (Harvey *et al.* 2005, 2011; Deibler and Kirschner 2010). In this mechanism, mitotic Cdk1 phosphorylates Swe1 in early mitosis, which activates Swe1 to bind and inhibit Cdk1. This initial phosphorylation, referred to as partial hyperphosphorylation, is opposed by PP2A so that a low level of Cdk1 activity escapes Swe1 inhibition to initiate early mitotic events, including assembly of the short

metaphase spindle. Further phosphorylation events in late mitosis lead to full hyperphosphorylation and inactivation of Swe1.

Mass spectrometry identified the inhibitory site on Cdk1 that is targeted by Swe1 (tyrosine 19) as the most strongly hyperphosphorylated site in *rts1*Δ cells (Zapata *et al.* 2014). Mass spectrometry also showed that Swe1 in *rts1*Δ cells is hyperphosphorylated on multiple sites that are known to play roles in Swe1 activation (Harvey *et al.* 2005). Furthermore, analysis of Swe1 phosphorylation has shown that Swe1 in *rts1*Δ cells persists in the partially hyperphosphorylated active form (Harvey *et al.* 2011). Finally, *rts1*Δ causes high levels of Cdk1 inhibitory phosphorylation and persistence of Cdk1 inhibitory phosphorylation in mitosis (Kennedy *et al.* 2016). Together, these observations suggest that Rts1-dependent control of Cdk1 inhibitory phosphorylation could play a major role in prolonging mitosis when growth is slowed in poor carbon.

The second candidate, Pds1/securin, inhibits chromosome segregation by binding and inhibiting separase, a protease that cleaves the cohesin proteins that hold chromosomes together (Cohen-Fix and Koshland 1997; Ciosk *et al.* 1998; Uhlmann *et al.* 1999). Exit from mitosis is triggered by activation of the anaphase-promoting complex (APC), which targets Pds1 for destruction. Pds1 and separase also influence the timing of mitotic cyclin destruction, which indicates that they can control the duration of mitosis (Cohen-Fix and Koshland 1999; Tinker-Kulberg and Morgan 1999). DNA damage induces a mitotic arrest by triggering signals that lead to phosphorylation of Pds1, thereby protecting it from the APC, and Pds1 and Swe1 appear to act redundantly to inhibit mitotic progression in response to DNA damage (Yamamoto *et al.* 1996; Wang *et al.* 2001; Palou *et al.* 2015). Thus, there are precedents for signals that work upstream of Pds1 and Swe1 to influence the duration of mitosis. Finally, proteome-wide mass spectrometry data suggest that Pds1 is hyperphosphorylated in *rts1*Δ cells (Zapata *et al.* 2014). In addition to inhibiting separase, Pds1 also promotes transport of separase into the nucleus. Thus, Pds1 plays both positive and negative roles in the regulation of separase.

Inhibitory phosphorylation of Cdk1 is partially responsible for the increased duration of mitosis in poor carbon

We first investigated the role of Cdk1 inhibitory phosphorylation. We hypothesized that the prolonged duration of mitosis and increased cell size caused by loss of Rts1 is due at least partly to hyperactive Swe1. To begin to test this, we first analyzed the effects of *swe1*Δ on the size of *rts1*Δ cells. The abnormally large size of *rts1*Δ cells was substantially reduced by *swe1*Δ, consistent with the idea that Swe1 is a major target of Rts1-dependent signals (Figure 2).

To test whether Swe1 plays a role in prolonging mitosis in poor carbon, we next tested whether Cdk1 inhibitory phosphorylation is prolonged in poor carbon. Cells growing in rich or poor carbon were released from a G1 arrest, and Cdk1

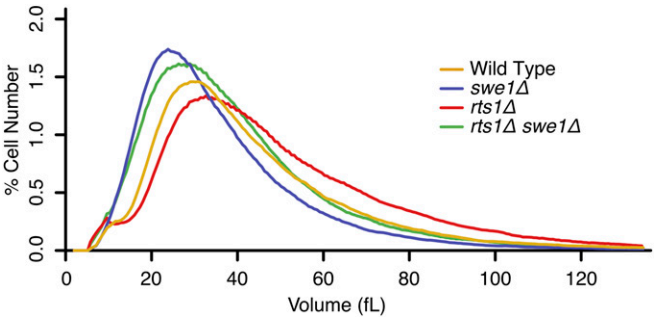

Figure 2 Swe1 and Pds1 influence cell size. Size distributions of log-phase populations of cells of the indicated genotypes were measured with a Coulter Counter. Cells were grown in YPD medium.

inhibitory phosphorylation was analyzed with a phospho-specific antibody. Samples were also analyzed by immunofluorescence to determine the fraction of cells with metaphase spindles at each time point. Cdk1 inhibitory phosphorylation was prolonged in poor carbon (Figure 3A). Moreover, metaphase spindles were present over a longer time interval in poor carbon and Cdk1 inhibitory phosphorylation was correlated with the presence of metaphase spindles. Together, these observations are consistent with a model in which Cdk1 inhibitory phosphorylation enforces a prolonged metaphase in poor carbon.

We also analyzed Swe1 phosphorylation during the cell cycle in rich and poor carbon. Phosphorylation of Swe1 during mitosis can be detected via electrophoretic mobility shifts (Sreenivasan and Kellogg 1999; Harvey *et al.* 2005, 2011). In rich carbon, Swe1 rapidly reached the fully hyperphosphorylated form that is thought to be required for its inactivation (Figure 3A). In poor carbon, Swe1 was present throughout much of the prolonged mitosis. Moreover, Swe1 took longer to reach the fully hyperphosphorylated form, and it persisted in the partially hyperphosphorylated form that is thought to represent an active form of Swe1 that restrains full activation of Cdk1 in early mitosis (Harvey *et al.* 2011). These observations suggest that signals that control Swe1 prolong Cdk1 inhibitory phosphorylation in poor nutrients.

The role of Swe1 was further characterized by analyzing daughter bud growth and mitotic events in single cells. In rich carbon, *swe1*Δ caused a slight reduction in the average duration of metaphase, as previously described (Figure 3B; see Figure S2A for dot plots and *P*-values) (Lianga *et al.* 2013). In poor carbon, *swe1*Δ caused a greater reduction in metaphase duration. Although *swe1*Δ reduced the duration of metaphase in poor carbon, it did not reduce it to the metaphase duration observed for wild-type cells in rich carbon, which indicated that the metaphase delay caused by poor carbon cannot be due solely to inhibitory phosphorylation of Cdk1. Loss of Swe1 had little effect on the duration of anaphase, consistent with the observation that Cdk1 inhibitory phosphorylation is observed primarily during metaphase (Figure 3A).

In both rich and poor carbon, *swe1*Δ caused reduced growth rate (Figure 3C). This, combined with the reduced duration of metaphase, caused *swe1*Δ daughter buds to

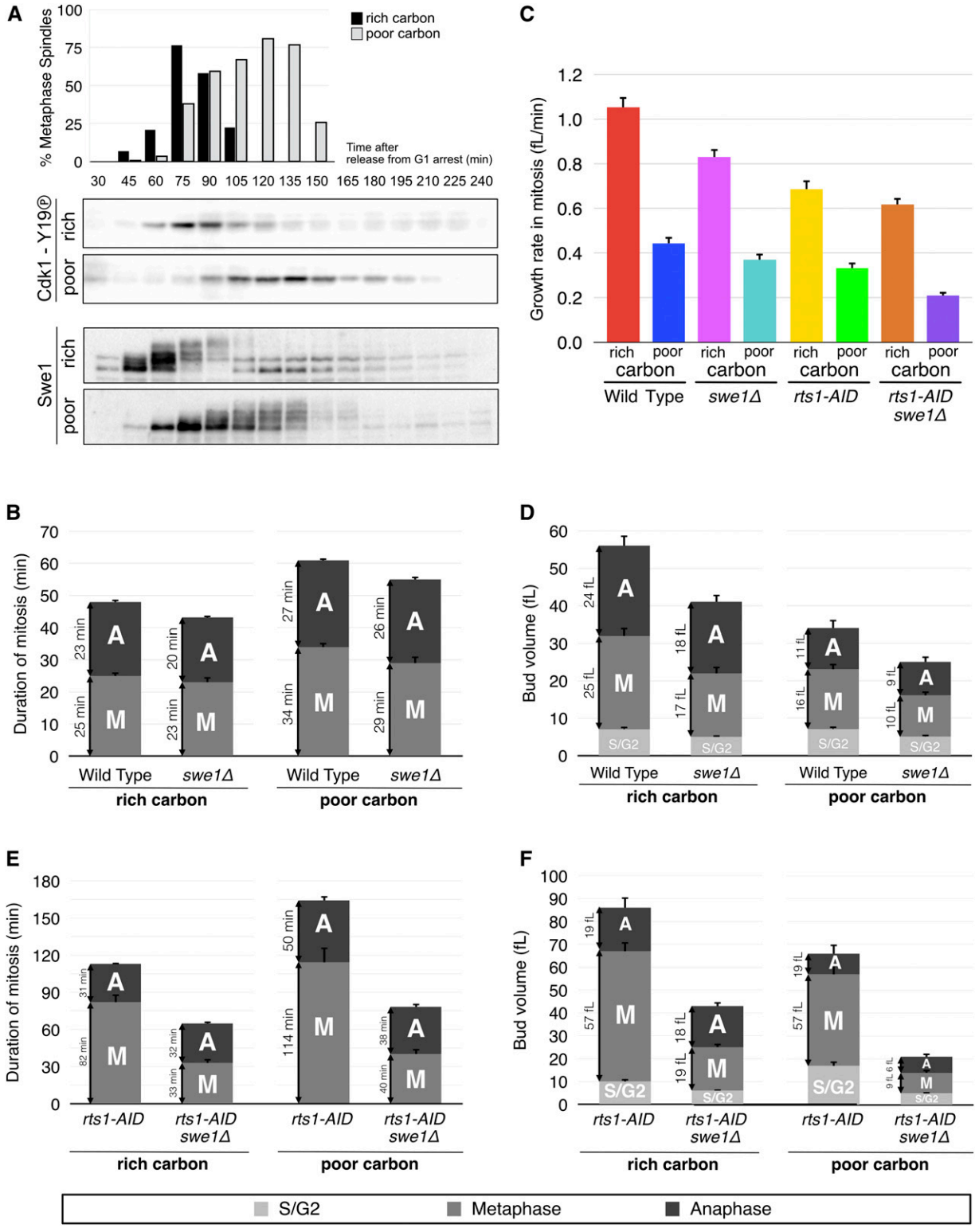

Figure 3 The increased duration of mitosis in poor carbon is partially due to Cdk1 inhibitory phosphorylation. (A) Wild-type cells growing in rich or poor carbon were released from a G1 arrest and samples were taken at 15-min intervals. The percentage of cells with a metaphase spindle was determined by immunofluorescence microscopy. Cdk1 inhibitory phosphorylation on tyrosine 19 was detected by western blot with a phospho-specific antibody. Swe1 was detected by western blot with an anti-Swe1 antibody. Cdk1 inhibitory phosphorylation and Swe1 were analyzed in the same samples. Mitotic spindle data are from an independent biological replicate that showed similar timing of events. (B) Average durations of metaphase and anaphase for wild-type and *swe1*Δ cells, growing in rich or poor carbon. (C) Average growth rates during metaphase and anaphase for wild-type and *swe1*Δ cells, in rich or poor carbon. (D) Average growth in volume during metaphase and anaphase for wild-type or *swe1*Δ cells, growing in rich or poor carbon. (E) Average durations of metaphase and anaphase for *rts1-AID* and *rts1-AID swe1*Δ cells, growing in rich or poor carbon. (F) Average growth in volume during metaphase and anaphase for *rts1-AID* and *rts1*-AID *swe1*Δ cells, growing in rich or poor carbon. Error bars represent SEM. A, anaphase; M, metaphase.

undergo mitotic transitions at a substantially reduced size in both rich and poor carbon (Figure 3D; see Figure S2, C and D for dot plots and *P*-values). Together, the data demonstrate that Swe1 plays a role in the increased duration of metaphase in poor carbon and is required for normal control of daughter cell size at cytokinesis. The reduced growth rate of daughter buds in *swe1*Δ cells could be due to the reduced size of their mother cells, since the growth rate of daughter cells is correlated with mother cell size (Leitao and Kellogg 2017).

We next defined the contribution of Cdk1 inhibitory phosphorylation to the mitotic delay observed in *rts1-AID* cells. Western blot assays confirmed that destruction of rts1-AID caused a prolonged mitotic delay in both rich and poor carbon (Figure S3A). The delay caused by *rts1-AID* in rich carbon was reduced, but not eliminated, by *swe1*Δ. We further discovered that *rts1*Δ caused a mitotic delay after release from a metaphase arrest. The delay was reduced by *swe1*Δ, but not fully eliminated (Figure S3B). In single-cell assays, the metaphase delays caused by *rts1-AID* in rich and poor carbon were reduced by *swe1*Δ, but not fully eliminated (Figure 3, B and E; see Figure S2A for dot plots and *P*-values). The increased duration of anaphase caused by *rts1-AID* in rich and poor carbon was largely unaffected by *swe1*Δ. Although *swe1*Δ did not fully rescue the mitotic delays caused by *rts1-AID*, it caused *rts1-AID* cells to exit mitosis at sizes similar to those of *swe1*Δ cells (Figure 3F; see Figure S2 for dot plots and *P*-values). This was a combined result of the reduction in mitotic duration and decreased growth rate in *rts1-AID swe1*Δ cells, relative to *rts1-AID* or *swe1*Δ cells.

Together, these observations demonstrate that nutrients and Rts1 influence mitotic duration and daughter cell size via a Swe1-dependent pathway, as well as by a Swe1-independent pathway. A previous study found that purified $PP2A^{Rts1}$ cannot dephosphorylate Swe1 *in vitro*, so it is likely that it controls Swe1 indirectly (Harvey *et al.* 2011). Another study suggested that it is possible that $PP2A^{Rts1}$ directly dephosphorylates Cdk1 (Kennedy *et al.* 2016).

Phosphorylation of Pds1 is controlled by nutrients and $PP2A^{Rts1}$

We next investigated the function and regulation of Pds1. Proteome-wide mass spectrometry analysis identified four serines in Pds1 that are hyperphosphorylated in *rts1*Δ cells (S185, S186, S212, and S213) (Zapata *et al.* 2014). Two of the sites (S212 and S213) were previously implicated in delaying mitosis in response to DNA damage (Wang *et al.* 2001). We hypothesized that hyperphosphorylation of Pds1 at these sites delays mitotic progression in poor carbon and in *rts1*Δ cells. To test this, we first used PhosTag gels to investigate how Pds1 phosphorylation responds to poor nutrients or to loss of Rts1. A greater fraction of Pds1 was found in hyperphosphorylated forms within 5 min of a shift to poor carbon (Figure 4A, lanes 1–3). Moreover, *rts1*Δ caused Pds1 to undergo more rapid and extensive hyperphosphorylation in response to poor carbon

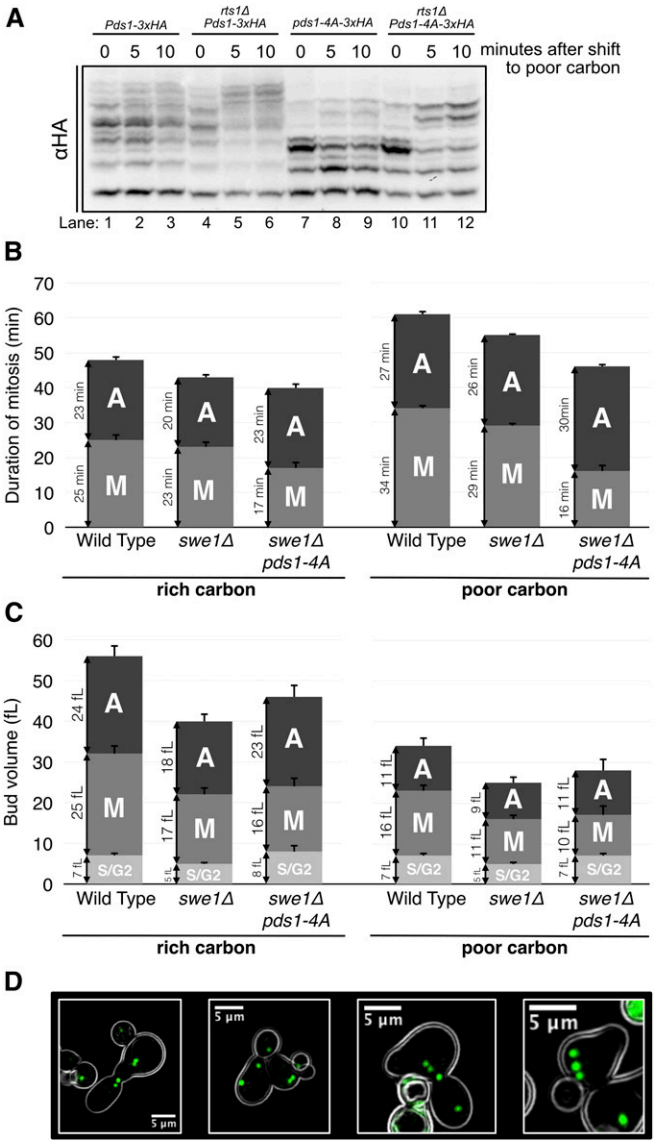

Figure 4 Pds1 and Swe1 are required for nutrient modulation of the duration of metaphase. (A) Wild-type, *rts1*Δ, and *pds1-4A* cells grown to log phase were switched from YPD to YPG/E and Pds1 phosphorylation was assayed by PhosTag western blot. (B) Average durations of metaphase and anaphase for wild-type, *swe1*Δ, and *swe1*Δ *pds1-4A* cells in rich or poor carbon. (C) Average growth in volume for all phases of the cell cycle except G1 phase for wild-type, *swe1*Δ, and *swe1*Δ *pds1-4A* cells in rich or poor carbon. (D) Examples of *swe1*Δ *pds1-4A* cells with multiple spindle poles. A, anaphase; M, metaphase.

(Figure 4A, lanes 4–6). A mutant version of Pds1 that lacks the four sites controlled by $PP2A^{Rts1}$ (*pds1-4A*) showed dramatically reduced hyperphosphorylation but retained a diminished response to poor carbon that was enhanced in *rts1*Δ cells, which suggests that there are additional Rts1-responsive sites that can undergo hyperphosphorylation in response to poor carbon (Figure 4A, lanes 7–9 and 10–12). These data shown that Pds1 undergoes rapid phosphorylation in response to changes in carbon source, and that Rts1 is required for normal control of Pds1 phosphorylation.

Pds1 and Swe1 are required for nutrient modulation of metaphase duration

To test whether phosphorylation of Pds1 contributes to the mitotic delay observed in *swe1*Δ cells in poor carbon, we analyzed the effects of *pds1-4A* on the durations of metaphase and anaphase in *swe1*Δ cells. Metaphase in *swe1*Δ *pds1-4A* cells was shorter than metaphase in *wild-type* cells or *swe1*Δ cells, in both rich and poor carbon (Figure 4B; see Figure S2A for dot plots and *P*-values). In addition, there was no difference in the duration of metaphase between rich and poor carbon in the *swe1*Δ *pds1-4A* cells. These data suggest that nutrient modulation of the duration of metaphase is dependent upon both Swe1 and Pds1.

*pds1-4A swe1*Δ cells growing in poor carbon completed metaphase at a reduced volume compared to *pds1-4A swe1*Δ cells growing in rich carbon (Figure 4C; see Figure S2C for dot plots and *P*-values). This was a consequence of reduced growth rate in poor carbon, since the duration of metaphase in *pds1-4A swe1*Δ cells was identical in rich and poor carbon. Thus, *pds1-4A swe1*Δ causes cell size at the completion of metaphase to become a simple function of growth rate, as originally imagined in early models of cell size control (Hartwell and Unger 1977). The duration of anaphase in *pds1-4A swe1*Δ cells was modulated by nutrients. In addition, the duration of anaphase and the extent of growth during anaphase were both increased in *pds1-4A swe1*Δ cells relative to *swe1*Δ cells. These observations suggest that the mechanisms that lengthen anaphase in response to carbon source are largely independent of Swe1 and phosphorylation of Pds1. The increased duration of anaphase in *pds1-4A swe1*Δ cells may reflect compensatory growth that occurs because the cells complete metaphase at an abnormally small size. Proteome-wide mass spectrometry identified numerous components of the mitotic exit network as potential targets of $PP2A^{Rts1}$-dependent regulation (Zapata *et al.* 2014). Thus, nutrient-dependent control of the mitotic exit network could account for the increased duration of growth in anaphase in poor nutrients. Alternatively, the anaphase delay could be a consequence of activation of the spindle position checkpoint in *pds1-4A swe1*Δ cells, although we observed no overt defects in spindle positioning (Chan and Amon 2009).

We also analyzed the effects of *pds1-4A* alone. The *pds1-4A* allele caused a large reduction in metaphase duration in rich carbon and a corresponding reduction in the extent of growth (Figure S4). We again observed what appears to be a compensatory increase in the duration of growth in anaphase in rich carbon. The *pds1-4A* allele had only a modest effect on the duration and extent of growth in metaphase in poor carbon, which suggests that Swe1 plays a more important role in the lengthening of metaphase in poor carbon.

The average size of *pds1-4A swe1*Δ buds at completion of anaphase in poor carbon was slightly larger than that of *swe1*Δ cells, which was due to a few very large outlier cells (see dot plots in Figure S2D). We noticed that some *pds1-4A swe1*Δ cells in poor carbon had more than two spindle pole bodies (Figure 4D). This suggested that they may be polyploid, which could be a consequence of a failure to undergo sufficient growth before nuclear division. Cells in which we could detect extra spindle poles, which constituted ~10% of the cells growing in poor carbon, were excluded from the analysis in Figure 4, B and C. However, the large outlier cells in the *pds1-4A swe1*Δ data could be polyploid cells that did not have well-separated spindle poles that would clearly identify them as having multiple nuclei. Since cell size scales with ploidy, the unusually large *pds1-4A swe1*Δ cells could correspond to polyploid cells. A previous study found that Swe1 and Pds1 act redundantly to prevent inappropriate chromosome segregation in response to DNA damage, which shows that Swe1 and Pds1 can work together to block chromosome segregation (Palou *et al.* 2015).

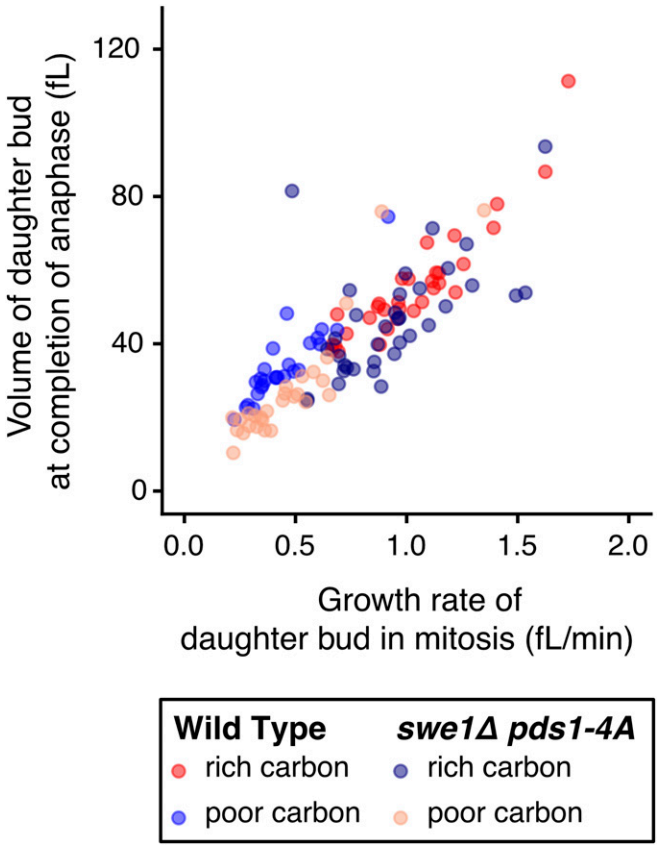

Figure 5 Pds1 and Swe1 are not required for the proportional relationship between cell size and growth rate. A plot of the volume of the daughter bud at completion of anaphase *vs.* growth rate during metaphase plus anaphase. Cells were grown in YPD medium.

A plot of cell size at completion of mitosis *vs.* growth rate revealed that *pds1-4A swe1*Δ cells have a reduced size, yet show a normal proportional relationship between cell size and growth rate (Figure 5). Thus, Swe1 and Pds1 do not appear to be required for the proportional relationship between cell size and growth rate.

Discussion

In previous work, we found that the duration and extent of growth in mitosis are strongly modulated by carbon source; however, the proteins that mediate modulation were unknown. Here, we show that nutrient modulation of cell growth and size in mitosis is dependent upon Rts1, and that both nutrients and Rts1 influence the duration and extent of growth in mitosis via Swe1 and Pds1. Rts1 is a well-characterized and highly conserved regulatory subunit for PP2A, so it is likely that Rts1 influences cell growth and size via the $PP2A^{Rts1}$ complex. However, Rts1 has also been reported to bind to PP1 in cells growing in poor carbon (Castermans *et al.* 2012), so it is possible that Rts1 also influences cell growth and size via PP2A-independent mechanisms.

The discovery that inactivation of Rts1 causes a failure in the proportional relationship between cell size and growth rate during mitosis provides further evidence that modulation of cell size at completion of mitosis is the result of active regulation, rather than a simple outcome of changes in growth rate. A previous study found that Ydj1, a conserved member of the DnaJ chaperone family, is required for the proportional relationship between cell size and growth rate in G1 phase (Ferrezuelo *et al.* 2012). Proteome-wide mass spectrometry data suggest that Ydj1 is regulated by $PP2A^{Rts1}$ (Zapata *et al.* 2014).

$PP2A^{Rts1}$ is embedded in a nutrient-modulated TORC2 signaling network that strongly influences cell growth and size (Lucena *et al.* 2018). Thus, it seems likely that the TORC2 network generates nutrient-dependent signals that influence cell growth and size in mitosis. Several previous observations are consistent with this idea. For example, decreased TORC2 signaling causes a decrease in the size of the smallest cells in a population, which represent newborn daughter cells that have just completed mitosis. In addition, cells that cannot produce ceramides, a key signaling output of the TORC2 network, show a large reduction in daughter cell size, as well as a complete failure in nutrient modulation of cell size (Lucena *et al.* 2018).

To explain the data, we suggest a model in which $PP2A^{Rts1}$ influences TORC2-dependent signals that enforce the proportional relationship between cell size and growth rate. Since the rate of growth in mitosis is proportional to cell size (Schmoller *et al.* 2015; Leitao and Kellogg 2017), one might expect that the signals that drive growth are also proportional to cell size and that there are mechanisms to ensure that the signals that set growth rate scale with size. In this case, a failure in a $PP2A^{Rts1}$-dependent mechanism that makes growth rate proportional to cell size should cause cells to grow at rates that are uncorrelated with size, leading to a loss of the correlation between cell size and growth rate. The correlation would break down in both directions: growth rate would no longer be proportional to cell size and cell size would no longer be proportional to growth rate. The fact that $PP2A^{Rts1}$ influences signaling within the TORC2 feedback loop suggests that it is well-positioned to enforce a mechanistic link between cell size and growth rate (Lucena *et al.* 2018). Moreover, there is evidence that the level of signaling in the feedback loop is influenced by growth, which might be expected for a signaling network that ensures that cell size and growth rate are proportional (Clarke *et al.* 2017; Alcaide-Gavilán *et al.* 2018). For example, one way to enforce a proportional relationship between cell size and growth rate would be to have the events of growth generate positive feedback signals that increase the rate of growth so that growth rate scales with size.

$PP2A^{Rts1}$-dependent signals that make cell size proportional to growth rate could also set the threshold amount of growth required for cell cycle progression. We imagine that Swe1 and Pds1 respond to growth-dependent signals that are used to measure cell size (Anastasia *et al.* 2012). $PP2A^{Rts1}$-dependent signals could set the strength of the growth-dependent signal required for cell cycle progression, which would ensure that cell size is matched to growth rate. More specifically, $PP2A^{Rts1}$-dependent signals could set the threshold level of growth-dependent signaling needed to trigger the removal of Cdk1 inhibitory phosphorylation or inactivation of Pds1. In this view, Swe1 and Pds1 would enforce the set point for cell size, but would not be required for the proportional relationship between cell size and growth rate.

A model in which the same global signals that set growth rate also set the critical amount of growth required for cell cycle progression would provide a simple mechanistic explanation for nutrient modulation of cell size. Since cell size control likely evolved as an outcome of growth control, it would make sense that control of cell growth and size are mechanistically linked. Further analysis of the signals that connect Pds1 and Swe1 to $PP2A^{Rts1}$, and the TORC2 network, should lead to important clues regarding how cell growth and size are controlled.

Acknowledgments

We thank Ben Abrams, Facilities Manager for the University of California, Santa Cruz Life Sciences Microscopy Center for support and mentoring with all microscopy-related techniques. R.M.L. was supported by a fellowship from the Fundação para a Ciência e a Tecnologia, with funds from the Programa Operacional Potencial Humano/Fundo Social Europeu, under the fellowship SFRH/BD/75004/2010. This work was supported by National Institutes of Health grant R01 GM-053959.

Literature Cited

Alcaide-Gavilán, M., R. Lucena, K. A. Schubert, K. L. Artiles, J. Zapata *et al.*, 2018 Modulation of TORC2 signaling by a conserved Lkb1 signaling axis in budding yeast. Genetics 210: 155–170. https://doi.org/10.1534/genetics.118.301296

Anastasia, S. D., D. L. Nguyen, V. Thai, M. Meloy, T. Macdonough *et al.*, 2012 A link between mitotic entry and membrane growth suggests a novel model for cell size control. J. Cell Biol. 197: 89–104. https://doi.org/10.1083/jcb.201108108

Artiles, K., S. Anastasia, D. McCusker, and D. R. Kellogg, 2009 The Rts1 regulatory subunit of protein phosphatase 2A is required for control of G1 cyclin transcription and nutrient modulation of

cell size. PLoS Genet. 5: e1000727. https://doi.org/10.1371/journal.pgen.1000727

Castermans, D., I. Somers, J. Kriel, W. Louwet, S. Wera *et al.*, 2012 Glucose-induced posttranslational activation of protein phosphatases PP2A and PP1 in yeast. Cell Res. 22: 1058–1077. https://doi.org/10.1038/cr.2012.20

Chan, L. Y., and A. Amon, 2009 The protein phosphatase 2A functions in the spindle position checkpoint by regulating the checkpoint kinase Kin4. Genes Dev. 23: 1639–1649. https://doi.org/10.1101/gad.1804609

Ciosk, R., W. Zachariae, C. Michaelis, A. Shevchenko, M. Mann *et al.*, 1998 An ESP1/PDS1 complex regulates loss of sister chromatid cohesion at the metaphase to anaphase transition in yeast. Cell 93: 1067–1076. https://doi.org/10.1016/S0092-8674(00)81211-8

Clarke, J., N. Dephoure, I. Horecka, S. Gygi, and D. Kellogg, 2017 A conserved signaling network monitors delivery of sphingolipids to the plasma membrane in budding yeast. Mol. Biol. Cell 28: 2589–2599.

Cohen-Fix, O., and D. Koshland, 1997 The anaphase inhibitor of Saccharomyces cerevisiae Pds1p is a target of the DNA damage checkpoint pathway. Proc. Natl. Acad. Sci. USA 94: 14361–14366. https://doi.org/10.1073/pnas.94.26.14361

Cohen-Fix, O., and D. Koshland, 1999 Pds1p of budding yeast has dual roles: inhibition of anaphase initiation and regulation of mitotic exit. Genes Dev. 13: 1950–1959. https://doi.org/10.1101/gad.13.15.1950

Deibler, R. W., and M. W. Kirschner, 2010 Quantitative reconstitution of mitotic CDK1 activation in somatic cell extracts. Mol. Cell 37: 753–767. https://doi.org/10.1016/j.molcel.2010.02.023

Elliott, S. G., and C. S. McLaughlin, 1978 Rate of macromolecular synthesis through the cell cycle of the yeast Saccharomyces cerevisiae. Proc. Natl. Acad. Sci. USA 75: 4384–4388. https://doi.org/10.1073/pnas.75.9.4384

Ferrezuelo, F., N. Colomina, A. Palmisano, E. Garí, C. Gallego *et al.*, 2012 The critical size is set at a single-cell level by growth rate to attain homeostasis and adaptation. Nat. Commun. 3: 1012. https://doi.org/10.1038/ncomms2015

Goranov, A. I., M. Cook, M. Ricicova, G. Ben-Ari, C. Gonzalez *et al.*, 2009 The rate of cell growth is governed by cell cycle stage. Genes Dev. 23: 1408–1422. https://doi.org/10.1101/gad.1777309

Hartwell, L. H., and M. W. Unger, 1977 Unequal division in Saccharomyces cerevisiae and its implications for the control of cell division. J. Cell Biol. 75: 422–435. https://doi.org/10.1083/jcb.75.2.422

Harvey, S. L., and D. R. Kellogg, 2003 Conservation of mechanisms controlling entry into mitosis: budding yeast wee1 delays entry into mitosis and is required for cell size control. Curr. Biol. 13: 264–275. https://doi.org/10.1016/S0960-9822(03)00049-6

Harvey, S. L., A. Charlet, W. Haas, S. P. Gygi, and D. R. Kellogg, 2005 Cdk1-dependent regulation of the mitotic inhibitor Wee1. Cell 122: 407–420. https://doi.org/10.1016/j.cell.2005.05.029

Harvey, S. L., G. Enciso, N. Dephoure, S. P. Gygi, J. Gunawardena *et al.*, 2011 A phosphatase threshold sets the level of Cdk1 activity in early mitosis in budding yeast. Mol. Biol. Cell 22: 3595–3608. https://doi.org/10.1091/mbc.e11-04-0340

Hirsch, J., and P. W. Han, 1969 Cellularity of rat adipose tissue: effects of growth, starvation, and obesity. The Journal of Lipid Research 10: 77–82.

Janke, C., M. M. Magiera, N. Rathfelder, C. Taxis, S. Reber *et al.*, 2004 A versatile toolbox for PCR-based tagging of yeast genes: new fluorescent proteins, more markers and promoter substitution cassettes. Yeast 21: 947–962. https://doi.org/10.1002/yea.1142

Johnston, G. C., J. R. Pringle, and L. H. Hartwell, 1977 Coordination of growth with cell division in the yeast Saccharomyces cerevisiae. Exp. Cell Res. 105: 79–98. https://doi.org/10.1016/0014-4827(77)90154-9

Johnston, G. C., C. W. Ehrhardt, A. Lorincz, and B. L. Carter, 1979 Regulation of cell size in the yeast Saccharomyces cerevisiae. J. Bacteriol. 137: 1–5.

Jorgensen, P., J. L. Nishikawa, B.-J. Breitkreutz, and M. Tyers, 2002 Systematic identification of pathways that couple cell growth and division in yeast. Science 297: 395–400. https://doi.org/10.1126/science.1070850

Kennedy, E. K., M. Dysart, N. Lianga, E. C. Williams, S. Pilon *et al.*, 2016 Redundant regulation of Cdk1 tyrosine dephosphorylation in Saccharomyces cerevisiae. Genetics 202: 903–910. https://doi.org/10.1534/genetics.115.182469

Leitao, R. M., and D. R. Kellogg, 2017 The duration of mitosis and daughter cell size are modulated by nutrients in budding yeast. J. Cell Biol. 216: 3463–3470. https://doi.org/10.1083/jcb.201609114

Lianga, N., E. C. Williams, E. K. Kennedy, C. Dore, S. Pilon *et al.*, 2013 A Wee1 checkpoint inhibits anaphase onset. J. Cell Biol. 201: 843–862. https://doi.org/10.1083/jcb.201212038

Longtine, M. S., A. McKenzie, D. J. DeMarini, N. G. Shah, A. Wach *et al.*, 1998 Additional modules for versatile and economical PCR-based gene deletion and modification in Saccharomyces cerevisiae. Yeast 14: 953–961. https://doi.org/10.1002/(SICI)1097-0061(199807)14:10<953::AID-YEA293>3.0.CO;2-U

Lucena, R., M. Alcaide-Gavilan, K. Schubert, M. He, M. G. Domnauer *et al.*, 2018 Cell size and growth rate are modulated by TORC2-dependent signals. Curr. Biol. 28: 196–210.e4. https://doi.org/10.1016/j.cub.2017.11.069

McCusker, D., C. Denison, S. Anderson, T. A. Egelhofer, J. R. Yates *et al.*, 2007 Cdk1 coordinates cell-surface growth with the cell cycle. Nat. Cell Biol. 9: 506–515. https://doi.org/10.1038/ncb1568

Nishimura, K., T. Fukagawa, H. Takisawa, T. Kakimoto, and M. Kanemaki, 2009 An auxin-based degron system for the rapid depletion of proteins in nonplant cells. Nat. Methods 6: 917–922. https://doi.org/10.1038/nmeth.1401

R Core Team. 2016. R: A language and environment for statistical computing. Available at https://www.gbif.org/tool/81287/r-a-language-and -environment-for-statistical-computing (Accessed September 15, 2017).

RStudio Team. 2015. RStudio: Integrated Development Environment for R. Available at http://www.rstudio.com. (Accessed: September 15, 2017).

Palou, G., R. Palou, F. Zeng, A. A. Vashisht, J. A. Wohlschlegel *et al.*, 2015 Three different pathways prevent chromosome segregation in the presence of DNA damage or replication stress in budding yeast. *PLoS Genet.* 11: e1005468. https://doi.org/10.1371/journal.pgen.1005468

Robertson, F. W., 1963 The ecological genetics of growth in Drosophila 6. The genetic correlation between the duration of the larval period and body size in relation to larval diet. Genetics Research 4: 74–92.

Raspelli, E., C. Cassani, E. Chiroli, and R. Fraschini, 2015 Budding yeast Swe1 is involved in the control of mitotic spindle elongation and is regulated by Cdc14 phosphatase during mitosis. J. Biol. Chem. 290: 6006. https://doi.org/10.1074/jbc.A114.590984

Schaechter, M., O. Maaloe, and N. O. Kjeldgaard, 1958 Dependency on medium and temperature of cell size and chemical composition during balanced grown of Salmonella typhimurium. J. Gen. Microbiol. 19: 592–606.

Schmoller, K. M., J. J. Turner, M. Kõivomägi, and J. M. Skotheim, 2015 Dilution of the cell cycle inhibitor Whi5 controls budding-yeast cell size. Nature 526: 268–272. https://doi.org/10.1038/nature14908

Shu, Y., H. Yang, E. Hallberg, and R. Hallberg, 1997 Molecular genetic analysis of Rts1p, a B′ regulatory subunit of Saccharomyces

cerevisiae protein phosphatase 2A. Mol. Cell. Biol. 17: 3242–3253. https://doi.org/10.1128/MCB.17.6.3242

Sreenivasan, A., and D. Kellogg, 1999 The elm1 kinase functions in a mitotic signaling network in budding yeast. Mol. Cell. Biol. 19: 7983–7994. https://doi.org/10.1128/MCB.19.12.7983

Tinker-Kulberg, R. L., and D. O. Morgan, 1999 Pds1 and Esp1 control both anaphase and mitotic exit in normal cells and after DNA damage. Genes Dev. 13: 1936–1949. https://doi.org/10.1101/gad.13.15.1936

Toledo, C. M., Y. Ding, P. Hoellerbauer, R. J. Davis, R. Basom *et al.*, 2015 Genome-wide CRISPR-Cas9 screens reveal loss of redundancy between PKMYT1 and WEE1 in glioblastoma stem-like cells. Cell Rep. 13: 2425–2439. https://doi.org/10.1016/j.celrep.2015.11.021

Tzur, A., R. Kafri, V. S. LeBleu, G. Lahav, and M. W. Kirschner, 2009 Cell growth and size homeostasis in proliferating animal cells. Science 325: 167–171.

Uhlmann, F., F. Lottspeich, and K. Nasmyth, 1999 Sister-chromatid separation at anaphase onset is promoted by cleavage of the cohesin subunit Scc1. Nature 400: 37–42. https://doi.org/10.1038/21831

Wang, H., D. Liu, Y. Wang, J. Qin, and S. J. Elledge, 2001 Pds1 phosphorylation in response to DNA damage is essential for its DNA damage checkpoint function. Genes Dev. 15: 1361–1372. https://doi.org/10.1101/gad.893201

Wickham, H. 2009. ggplot2: Elegant Graphics for Data Analysis. New York: Springer-Verlag.

Winey, M., and E. T. O'Toole, 2001 The spindle cycle in budding yeast. Nat. Cell Biol. 3: E23–E27. https://doi.org/10.1038/35050663

Yamamoto, A., V. Guacci, and D. Koshland, 1996 Pds1p is required for faithful execution of anaphase in the yeast, Saccharomyces cerevisiae. The Journal of Cell Biology 133: 85–97.

Zapata, J., N. Dephoure, T. Macdonough, Y. Yu, E. J. Parnell *et al.*, 2014 PP2ARts1 is a master regulator of pathways that control cell size. J. Cell Biol. 204: 359–376. https://doi.org/10.1083/jcb.201309119

Communicating editor: O. Cohen-Fix